

# We are IntechOpen, the world's leading publisher of Open Access books Built by scientists, for scientists

4,800

Open access books available

122,000

International authors and editors

135M

Downloads

Our authors are among the

154

Countries delivered to

TOP 1%

most cited scientists

12.2%

Contributors from top 500 universities



WEB OF SCIENCE™

Selection of our books indexed in the Book Citation Index  
in Web of Science™ Core Collection (BKCI)

Interested in publishing with us?  
Contact [book.department@intechopen.com](mailto:book.department@intechopen.com)

Numbers displayed above are based on latest data collected.  
For more information visit [www.intechopen.com](http://www.intechopen.com)



---

# Heat Transfer of Helix Energy Pile: Part 1: Traditional Cylinder Helix Energy Pile

---

Guangqin Huang, Yajiao Liu, Xiaofeng Yang and Chunlong Zhuang

Additional information is available at the end of the chapter

<http://dx.doi.org/10.5772/intechopen.76820>

---

## Abstract

Helix energy pile (HEP) is a new popular ground heat exchanger that has the advantages of large heat exchange rate and low initial cost. As for the traditional helix energy pile, the tube is wound on the cylindrical wall, which is called the cylinder helix energy pile (CyHEP). Further, both analytical solution model and numerical solution model for CyHEP are built to discuss the dynamic characteristics of thermal interferences and heat transfer performance. The results indicate that four heat exchange stages for the spiral pile geothermal heat exchanger along the fluid flow direction are revealed: inlet heat exchange stage, grout thermal short-circuiting stage, small temperature difference stage and outlet heat exchange stage. Each stage has corresponding heat transfer characteristics, and reducing the length of small temperature difference stage and increasing the other stages would enhance the heat exchange of spiral geothermal ground heat exchanger. As the pile diameter increases, the heat transfer per unit tube length decreases, and the heat exchange per unit pile depth increases. As the pile depth increases, the heat transfer per unit tube length and the heat exchange per unit pile depth are reduced. And as the pitch increases, the heat transfer per unit tube length increases, and the heat exchange per unit pile depth decreases.

**Keywords:** cylinder, helix energy pile, analytical, numerical, thermal interferences, stages

---

## 1. Introduction

Energy saving and environmental protection have been the symbols in modern development. In China, “Strategic Action Plan for Energy Development (2014–2020)” was published in November 2014 in order to achieve sustainable development. The plan points out that the

---

non-fossil energy share of primary energy consumption would reach 15% by 2020 and the utilized quantity of geothermal energy would run up to 50 million tons of standard coal. Ground source heat pump (GSHP) is an efficient technology to exploit the shallow geothermal energy and has been applied extensively in building energy conservation.

GSHP utilizes the ground maintaining a nearly constant temperature as the heat source or sink, and the particular underground temperature is appropriate for efficient operation of the unit. The most important component for GSHP is the ground heat exchanger (GHE) and the borehole GHE with U-type tube. However, the high installation and drilling cost restrict the application of borehole GHE, especially for rocky areas. Therefore, energy piles [1] have been proposed and widely applied for its good economic and well-heated transfer performance. The primary structure forms of energy piles consisting of U type [2–4] (such as single U type, parallel double U type, triple U type and series U type) and helix type [5–7] and the helix energy piles (HEPs) are promising GHEs due to the characteristics of large heat exchange rate and no air choking in the pipes. However, due to the features of complex helix structures, shallow burial and a large diameter of the pile, the heat transfer characteristics of HEPs are completely different from the U-type borehole GHE and would not be described by classical Kelvin's line source. Hence, the heat transfer of HEP has formed an academic focus.

## 2. Heat transfer model and characteristics of the traditional cylinder helix energy pile (CyHEP)

Helix energy pile is a new kind of heat exchanger for ground source heat pump. It is usually buried in the building concrete pile foundation, combined with the building structure. Compared with the conventional U-type and W-type energy pile, helix energy pile has a larger heat transfer area under the same depth. In addition, helix energy pile can avoid the problem of air accumulation at the top of U-type and W-type ones. As for the traditional helix energy pile, the tube is wound on the cylindrical wall as shown in **Figure 1**, which is called the cylinder helix energy pile (CyHEP) in this section.

### 2.1. Heat transfer model

Through literature research and analysis, it was found that due to the complicated structure of the cylinder helix energy pile, and there is a lack of research on the heat transfer model of it. At present, the heat transfer model is mainly a thermal conductivity model. It is considered that the thermo-physical properties of the pile backfill are the same as those of the soil, which is different from the actual heat transfer process. Most of the numerical solution models are simulated with commercial CFD software. However commercial CFD software has modeling and meshing difficulties, poor flexibility and other shortcomings. Based on the above reasons, a new discrete method of cylinder helix energy pile is presented in this section, and a three-dimensional numerical heat transfer model is established based on a transient heat balance theory. It can provide a more accurate description of the heat transfer process of the cylinder helix energy pile, thus providing design guidance for the actual project.

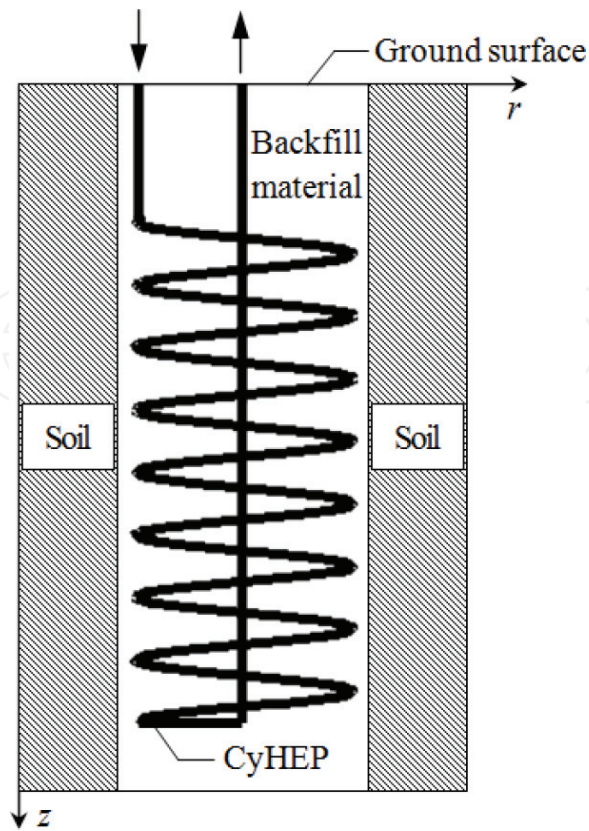


Figure 1. Cylinder helix energy pile (CyHEP).

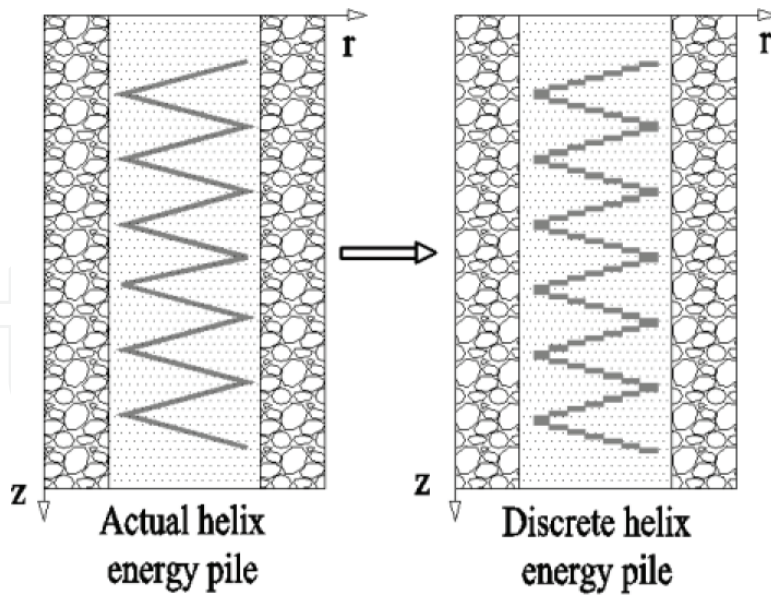


Figure 2. The sketch of discretized helix energy pile.

Figure 2 shows the sketch of a discretized helix energy pile. As shown in the figure, the continuous, circular cross-section helical fluid is discretely divided into a finite number of discrete, non-continuous stepped and square cross-section cells. The shape of a single fluid cell

is shown in **Figure 3**, which is a micro-cell under the cylindrical coordinate system. In this way, the discrete fluid unit body can be better combined with the cylindrical coordinate system to facilitate the establishment of the heat balance equation of the fluid unit body, the backfill material and the geotechnical unit body.

Taking each discrete element as the research object, the amount of energy change per unit time of the element is equal to the net amount of heat transferred from the adjacent element, which is the essence of the transient heat balance principle of the element. As shown in **Figure 4**, within a certain period of time, the transient thermal equilibrium equation of the unit body is shown as the following:

$$q_{z+} + q_{z-} + q_{r+} + q_{r-} + q_{\theta+} + q_{\theta-} = \rho c_p V(i, j, k) \frac{T(i, j, k, \tau + 1) - T(i, j, k, \tau)}{\tau_{sp}} \quad (1)$$

where  $q_{z+}$ ,  $q_{z-}$  are heat flux transferred from the unit below and above in the  $z$  direction to the calculated unit,  $W/m^2$ ;  $q_{r+}$ ,  $q_{r-}$  are heat fluxes transferred from the unit in the radial positive normal direction and the negative normal direction to the calculated unit,  $W/m^2$ ;  $q_{\theta+}$ ,  $q_{\theta-}$  are heat fluxes transferred from the unit in the positive normal of  $\theta$  direction and the negative normal of  $\theta$  direction to the calculated unit,  $W/m^2$ ;  $\rho$  is the density of the calculated unit,  $kg/m^3$ ;  $c_p$  is the specific heat of the calculated unit,  $J \cdot m^{-3} \cdot ^\circ C^{-1}$ ;  $V(i, j, k)$  is the volume of the calculated

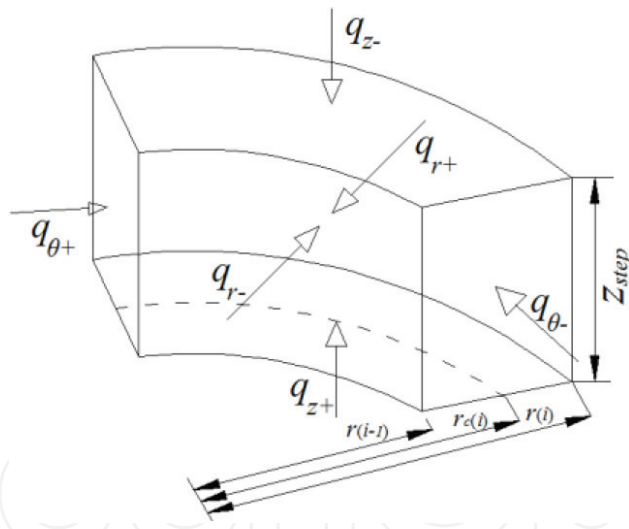


**Figure 3.** The sketch of the heat balance of unit body.

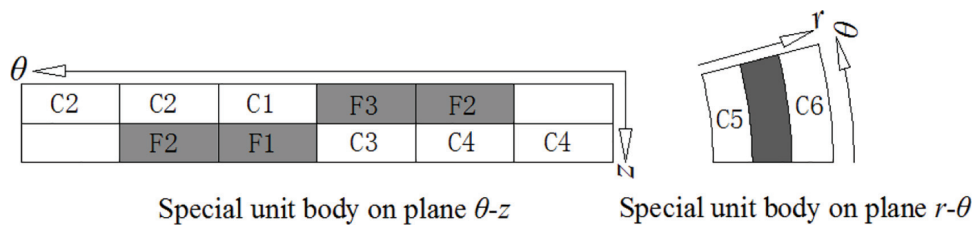


**Figure 4.** The sketch of the positional relation of special unit body.

unit,  $V(i,j,k) = z_{sp} \cdot [0.5\theta_{sp}(j) (r^2(i) - r^2(i - 1))]$ ,  $m^3$ ;  $\theta_{sp}$  is the increment in  $\theta$  direction;  $\tau_{sp}$  is the time step,  $s$ ;  $T$  is the temperature,  $^{\circ}C$ .

It is the key for the principle of transient heat balance to determine the heat transfer  $q$  between adjacent unit bodies in Eq. (1). And the heat transfer  $q$  between adjacent unit bodies is determined by the temperature difference and thermal resistance of adjacent unit bodies as shown in Eq. (2):

$$\begin{cases} q_{z+} = \frac{T(i,j,k+1) - T(i,j,k)}{R_{z+}} & q_{r+} = \frac{T(i+1,j,k) - T(i,j,k)}{R_{r+}} & q_{\theta+} = \frac{T(i,j+1,k) - T(i,j,k)}{R_{\theta+}} \\ q_{z-} = \frac{T(i,j,k-1) - T(i,j,k)}{R_{z-}} & q_{r-} = \frac{T(i-1,j,k) - T(i,j,k)}{R_{r-}} & q_{\theta-} = \frac{T(i,j-1,k) - T(i,j,k)}{R_{\theta-}} \end{cases} \quad (2)$$

where  $R_{z+}$ ,  $R_{z-}$  is the heat transfer resistance between the unit below and above in the  $z$  direction and the calculated unit,  $^{\circ}C \cdot m^2 \cdot W^{-1}$ ;  $R_{r+}$ ,  $R_{r-}$  is the heat transfer resistance between the unit in the radial positive normal direction and the negative normal direction and the calculated unit,  $^{\circ}C \cdot m^2 \cdot W^{-1}$ ;  $R_{\theta+}$ ,  $R_{\theta-}$  is the heat transfer resistance between the unit in the positive normal of  $\theta$  direction and the negative normal of  $\theta$  direction and the calculated unit,  $^{\circ}C \cdot m^2 \cdot W^{-1}$ .

In sum, for the three-dimensional heat transfer model proposed in this section, the key lies in the calculation of heat flow or thermal resistance, and the heat flow and thermal resistance for different types of unit bodies are determined, respectively.

(1) Thermal resistance calculation for unit body not in contact with the fluid: As for the unit body not in contact with the fluid, the heat transfer is a pure thermal conduction process; thus, the thermal resistance in the  $z$  direction,  $r$  direction and  $\theta$  direction can be calculated as following:

$$R_{z+} = R_{z-} = \frac{2z_{sp}}{\lambda_s \theta_{sp}(j) (r^2(i) - r^2(i - 1))} \quad (3)$$

$$R_{r+} = \frac{1}{\lambda_s \theta_{sp}(j) z_{sp}} \ln \left[ \frac{r_c(i+1)}{r_c(i)} \right] \quad (4)$$

$$R_{r-} = \frac{1}{\lambda_s \theta_{sp}(j) z_{sp}} \ln \left[ \frac{r_c(i)}{r_c(i-1)} \right] \quad (5)$$

$$R_{\theta+} = \frac{(\theta_{sp}(j+1) + \theta_{sp}(j)) r_c(i)}{2\lambda_s z_{sp} (r(i) - r(i-1))} \quad (6)$$

$$R_{\theta-} = \frac{(\theta_{sp}(j) + \theta_{sp}(j-1)) r_c(i)}{2\lambda_s z_{sp} (r(i) - r(i-1))} \quad (7)$$

where  $\lambda_s$  is the thermal conductivity of soil,  $W \cdot m^{-1} \cdot ^{\circ}C$  and  $r_c(i)$  is the distance from center of calculated unit to center of the pile,  $m$ .

(2) Thermal resistance calculation for unit body in contact with fluid: For the unit body in contact with fluid, as shown in **Figure 4**, the heat transfer resistance of C1 and C6 units should include three items: fluid convection thermal resistance, thermal conductivity resistance of the

wall and thermal conductivity resistance of the backfills. Thus, for a typical unit body C2, the thermal resistance in the  $z$  direction can be calculated as the following and the other thermal resistances of unit body C2 can be calculated in the same way as thermal resistance calculation for unit body not in contact with the fluid. In the same way, the calculation methods of the thermal resistances of the unit bodies C1 and C3–C6 in contact with the fluid are similar to those of the unit body C2.

$$R_{z+} = \frac{2(0.5z_{sp} - \delta)}{\lambda_g \theta_{sp}(j)(r^2(i) - r^2(i-1))} + \frac{2\delta}{\lambda_p \theta_{sp}(j)(r^2(i) - r^2(i-1))} + \frac{2}{h \cdot \theta_{sp}(j)(r^2(i) - r^2(i-1))} \quad (8)$$

where  $\lambda_g$  is the thermal conductivity of the backfill,  $W \cdot m^{-1} \cdot ^\circ C$ ;  $\delta$  is the spiral wall thickness,  $m$ ;  $h$  is the convection heat transfer coefficient inside the tube,  $W \cdot m^{-2} \cdot ^\circ C^{-1}$ .

(3) Heat flow calculation for fluid unit: Due to the discretized fluid cell body being in the form of stairs, in terms of geometry, the upper ladder cell body (cell F3 in **Figure 4**) and the lower ladder cell body (cell F1 in **Figure 4**) fail to ensure the continuity of flow and heat transfer. Therefore, in order to ensure continuity, it is assumed that the upper fluid unit F3 and the lower fluid unit F1 have a thermal effect, and the fluid unit F3 and the backfilling unit C1 and the fluid unit F1 and the backfilling unit C3 are insulated. Based on the above assumptions, the expression of heat flow in the  $\theta$  direction of the fluid units F3 and F2 can be obtained as shown in Eq. (9). And heat transfer resistance in other directions is determined by the calculation of the thermal resistance of the unit in contact with the fluid. For the F1 fluid unit, in order to ensure the continuity of the fluid,  $q_{\theta-}$  should be the heat transferred from unit F3 to unit F1, and it is calculated in the same way as unit F3 and unit F2.

$$\begin{cases} q_{\theta+} = -mc_{p,f}T(i, j, k, \tau) \\ q_{\theta-} = mc_{p,f}T(i, j - 1, k, \tau) \end{cases} \quad (9)$$

where  $m$  is the fluid flow,  $m^3 \cdot s^{-1}$  and  $cp,f$  is the fluid specific heat,  $J \cdot m^{-3} \cdot ^\circ C^{-1}$ .

(4) Soil surface boundary condition: As the helix energy pile is shallow, pile depth is generally about 10 m; the soil surface environmental factors, such as air temperature, will affect the soil temperature of the pile foundation, thus affecting its heat transfer performance. For pile foundations installed in the basement, this section ignores the radiative heat transfer between the ground and other surfaces in the basement. And considering the convective heat transfer between the ground and the air, the boundary conditions of the soil surface are given by Eq. (10).

$$q_{z-} = (T_a(\tau) - T(i, j, 0, \tau))h_a A(i, j, 0) \quad (10)$$

where  $A(i, j, 0)$  is the top surface area of the unit  $(i, j, 0)$ ,  $A(i, j, 0) = \theta_{sp}(r(i)^2 - r(i-1)^2)$ ,  $m^2$ ;  $h_a$  is the convection heat transfer coefficient,  $W \cdot m^{-2} \cdot ^\circ C^{-1}$  and  $T_a$  is the air temperature,  $^\circ C$ .

Then the heat flow or thermal resistance formula of each type of unit body above is brought into the heat balance, Eq. (1), and the linear equations of the temperature field of helix energy pile at time  $\tau$  can be obtained. The temperature field of fluid and heat transfer area is calculated

with the C# programming language in the visual studio program developed platform, using the Gauss–Seidel iterative method. This is the three-dimensional numerical heat transfer model established in this section based on transient heat balance theory. It can provide more accurate description of the heat transfer process of the cylinder helix energy pile, thus providing design guidance for the actual project.

## 2.2. Heat transfer characteristic along the pipe

For helix energy piles, the heat transfer along the pipe and the geothermal temperature distribution characteristics are of great significance to the optimal design of the heat exchangers. The engineering significance of pitch, pile diameter, flow rate and other design parameters can be obtained from the perspective of efficient heat transfer. Based on the establishment of the three-dimensional numerical heat transfer model of the helix energy pile mentioned above, this section analyzes the fluid heat transfer along the pipe and geothermal temperature distribution characteristics and lays a theoretical foundation for its optimization design.

For helix energy piles, since the fluid flows downward along the tube length spirally in the spiral tube, the general direction of the fluid flow is vertically downward; there is no “reverse” flow between the fluids, the fluid temperature in the tube has the characteristic of gradually decreasing or increasing along the flow direction of the tube. And according to the geometric characteristics of the helix energy pile, the spiral pipe is divided into four stages of heat transfer along the process, as shown in **Figure 5**.

1. Entrance stage (L1): In the vicinity of the inlet part of the helix pipe, the top of the pipe is in direct contact with the covered area, and there is no heat exchange pipe in the covered area. In addition to transferring heat (cold) in the radial direction, fluid in the pipe also transfers heat (cold) to the covered area in the axial direction, so this stage has a larger heat exchange capacity. However, as the flow progresses, the distance between the helical fluid and the covered area is further away; the axial heat transfer gradually decreases, and the thermal short circuit between the adjacent spiral coils in the axial direction becomes stronger and stronger. The heat transfer efficiency gradually decreases, resulting in a gradual decline in heat transfer. Define the above stage as the entrance stage; the heat exchanger length is L1.
2. Thermal short circuit stage (L2): With the increase of the distance along the pipeline, the entrance stage is over; the phenomenon of thermal short circuit between adjacent spiral pipes in the axial direction is serious, and the amount of cold (heat) emitted from the spiral fluid in the axial direction to the soil is less and less. The amount of cold (heat) is mainly transmitted in the diameter direction. Due to the limited volume of the backfill area and the large temperature difference between the fluid in the initial stage of the spiral pipe and the surrounding soil/backfill, the intensity of the heat transfer is relatively large and the amount of cold (heat) emitted to the backfill area aggregates, resulting in the backfill area being short circuited seriously in the diameter direction, and this part is defined as the thermal short circuit stage; the length is L2. At this stage, it has the following salient



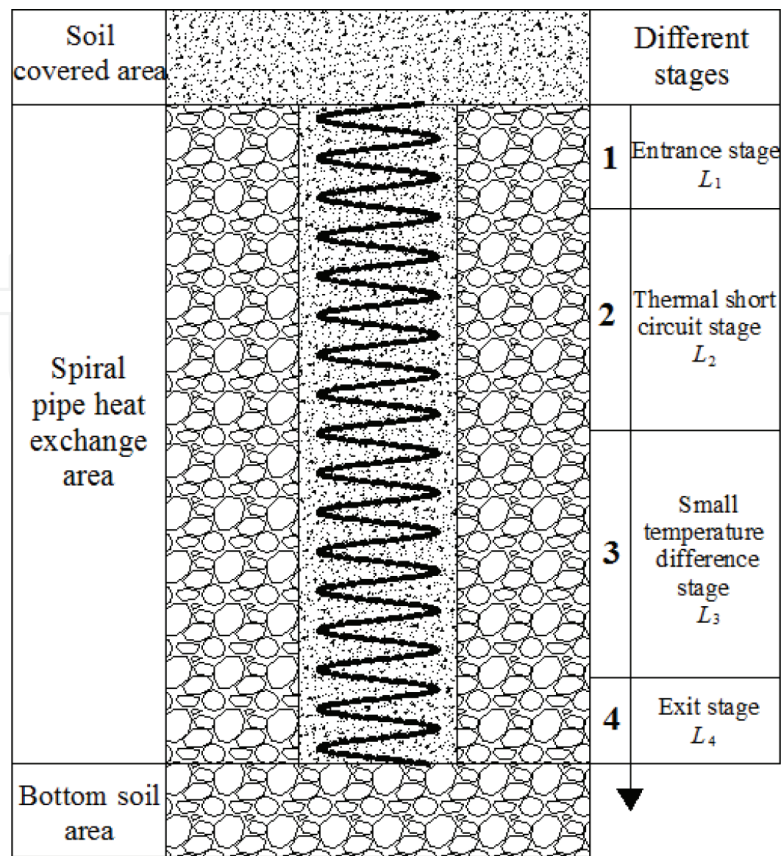


Figure 5. Heat transfer characteristic along the pipe.

features: the thermal short circuit effect in the diameter direction of the backfill area and the axial thermal short circuit effect are serious, but the thermal short circuit phenomenon in the diameter direction of the backfill area is gradually weakened and the heat exchange capacity gradually increases.

3. Small temperature difference stage ( $L_3$ ): When the thermal short circuit stage is over, the thermal short circuit phenomenon in the backfill area will be weak and the fluid temperature will decrease or increase further, resulting in lower heat transfer temperature difference between the fluid and the surrounding area; thus, the heat exchange capacity of the heat exchanger is gradually reduced. This stage is defined as the small temperature difference stage and the length is  $L_3$ . This stage has the following salient features: temperature difference between fluid and rock and soil is small, capacity of geothermal storage (heat) is weak and heat transfer capacity gradually decreases.
4. Exit stage ( $L_4$ ): As the small temperature difference stage is over, the fluid is close to the outlet part of the helix pipe. This stage is defined as the exit stage and its length is  $L_4$ . The exit stage is similar to the entrance stage. Since the spiral pipe near the exit is in direct contact with the soil at the bottom of the buried pipe, the axial thermal short circuit effect is weak. In addition to the heat exchange in the diameter direction, the fluid in the pipe also exchanges heat with the soil at the bottom of the ground tube. And as the fluid flows along

the pipe, the distance between the spiral fluid and the bottom of the soil gradually shortens, the axial thermal short circuit effect becomes weak; thus, the heat transfer capacity gradually increases.

Taking the case of summer heat release condition as an example, under the condition of constant inlet water temperature, the proposed three-dimensional numerical heat transfer model is used to simulate the fluid and soil temperature of the cylinder helix energy pile. And the four stages defined above are discussed. The main parameters of simulation are shown in **Table 1**. According to the thermo-physical properties of dense clay, the thermal conductivity of rock and soil is  $1.2 \text{ W}/(\text{m}\cdot^\circ\text{C})$  and the specific heat of volume is  $1680 \text{ kJ}/(\text{m}^3\cdot^\circ\text{C})$ . The thermal conductivity of backfilling material is  $1.5 \text{ W}/(\text{m}\cdot^\circ\text{C})$ , the specific heat of volume is  $2200 \text{ kJ}/(\text{m}^3\cdot^\circ\text{C})$  and the thermal conductivity of the spiral pipe is  $0.45 \text{ W}/(\text{m}\cdot^\circ\text{C})$ .

**Figure 6** shows the temperature distribution of the fluid at  $\tau = 48 \text{ h}$ . It can be seen from the figure that the temperature of the fluid decreases gradually along the length of the pipe. The rate of change of fluid temperature at the entrance and exit stages is obviously larger, indicating that at the inlet and outlet heat transfer stage, the axial heat transfer is more prominent.

Parameters	Unit	Value
Inlet water temperature	$^\circ\text{C}$	35
Water flow rate	m/s	0.3
Running time	h	48
Cover soil depth	m	2
Buried depth of the pile	m	8
Diameter of the pile	m	1.5
Pitch	m	0.15

**Table 1.** Main parameters of simulation.

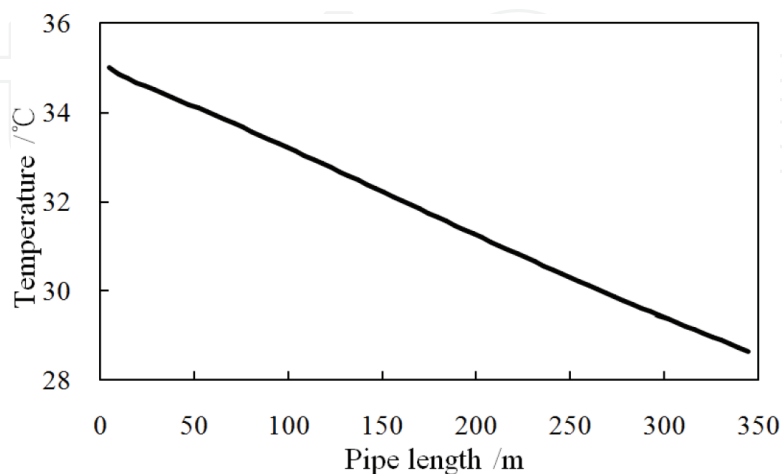


**Figure 6.** Fluid temperature distribution along the flow direction.

Figure 7 and Figure 8 show the changes of fluid heat transfer along the pipe and the vertical geothermal temperature distribution; we can clearly distinguish the four heat transfer stages proposed above.

1. Entrance stage (0–30 m): According to the vertical geothermal temperature field given in Figure 8, it can be seen that the soil temperature in the affected area at this stage has a large temperature gradient in the axial and radial directions, resulting in a significantly larger

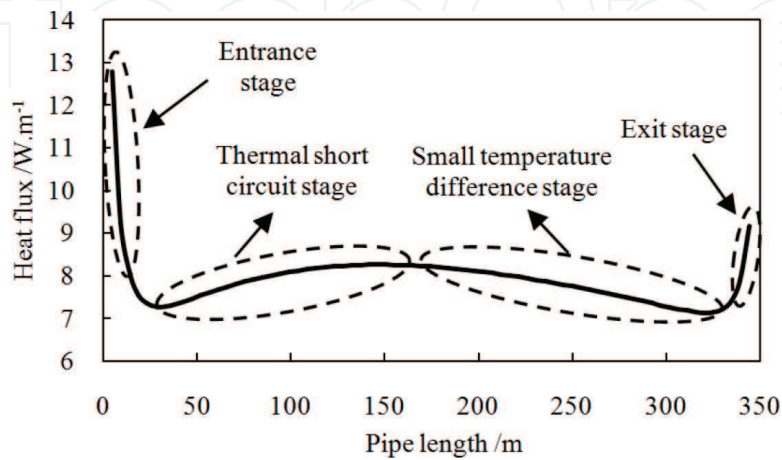


Figure 7. Fluid heat flux along the flow direction.

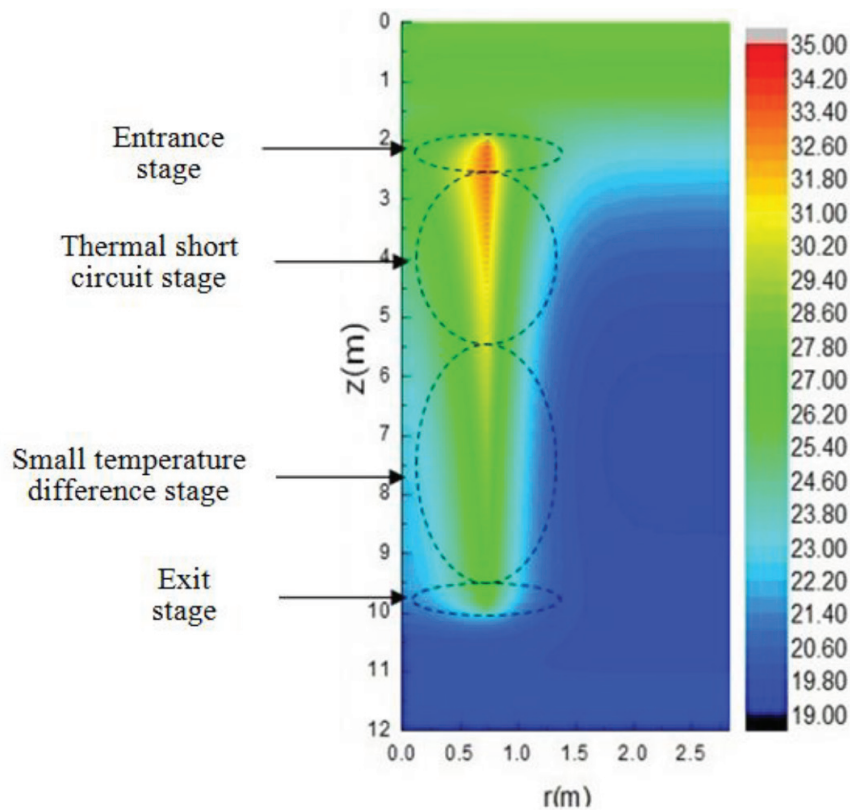


Figure 8. Temperature field on r-z plane.

heat transfer at this stage. However, as the distance between the fluid and the covered area increases, the axial thermal interference between the adjacent spiral coils increases and the amount of heat exchange decreases rapidly.

2. Thermal short circuit stage (30–150 m): Due to the high fluid temperature at this stage, a large amount of heat is transferred to the backfill area and the volume of the backfill area is limited, resulting in the accumulation of heat in the backfill area with high temperature and strong thermal short circuit effect in the diameter direction of the backfill area. However, as shown in **Figure 8**, with the gradual increase of the distance along the distance, the temperature in the backfill zone gradually decreases; the thermal influence in the backfill area decreases, the thermal effect radius decreases, the thermal short circuit effect gradually decreases and the heat transfer capacity gradually increases.
3. Small temperature difference stage (150–320 m): After the heat exchange at the entrance and thermal short circuit stages, the fluid temperature is lower and the heat transfer temperature difference between the fluid and the surrounding heat transfer area is gradually reduced, and the effect of cold (heat) storage in the soil is poor, resulting in the decrease of heat transfer capacity at this stage.
4. Exit stage (320–344 m): This stage is similar to the entrance stage. The fluid is in direct contact with the soil at the bottom of the spiral pipe. The soil temperature has a large temperature gradient both in radial direction and in axial direction, and the heat transfer effect is better. With the increase of the distance along the path, the closer the distance between the spiral fluid and the bottom soil, the more obvious the axial heat transfer effect is, and the heat transfer capacity gradually increases.

It can be seen from the analysis of the four stages that the entrance stage, thermal short circuit stage and exit stage belong to certain stages, and these three stages are beneficial for the whole heat exchange, especially for the entrance and exit stage; the heat transfer capacity is higher than the thermal short circuit and small temperature difference stages. For the small temperature difference stage, the heat transfer capacity decreases along the pipe length, so in the actual project design, it is necessary to reduce the proportion of the small temperature difference stage to the total heat exchange tube length and to maximize the other three stages, especially the entrance and exit stages.

### 2.3. Heat transfer capacity analysis

Based on the proposed three-dimensional numerical heat transfer model, this section analyzes and discusses the influence of different design parameters (pile diameter, pile depth and pitch) on cylinder helix energy pile, providing effective and direct theoretical guidance for the actual project.

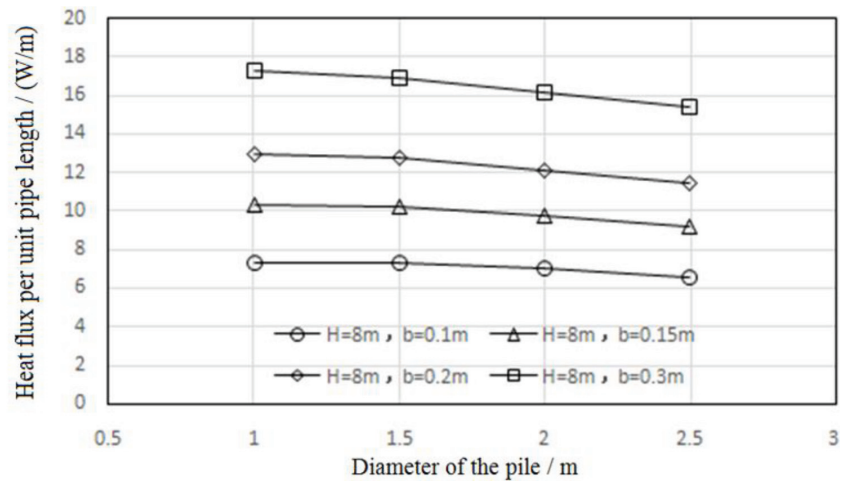
#### 2.3.1. Simulation conditions

The method of constant inlet water temperature is adopted to analyze and discuss the heat exchange capacity of the cylinder helix energy pile. The inlet temperature is 35°C and the flow

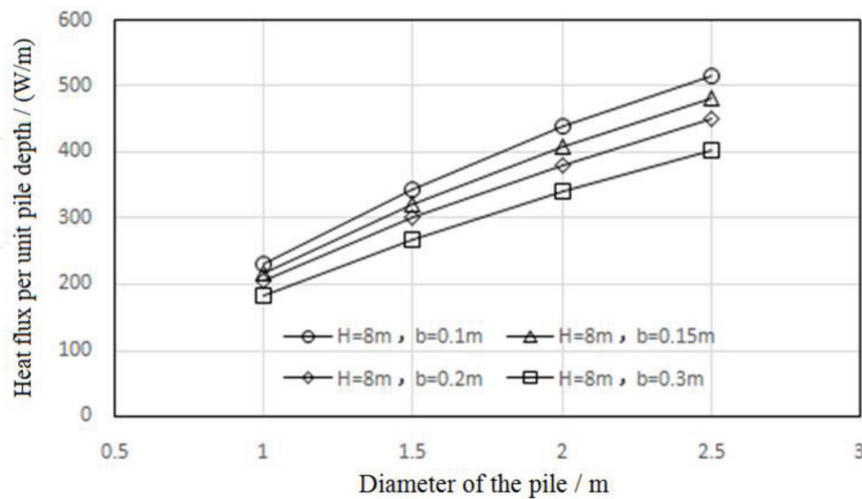
rate is 0.3 m/s. According to the thermo-physical properties of dense clay, the thermal conductivity of rock and soil is  $1.2 \text{ W}/(\text{m}\cdot^\circ\text{C})$  and the volumetric specific heat is  $1680 \text{ kJ}/(\text{m}^3\cdot^\circ\text{C})$ . The thermal conductivity of backfill material is  $1.5 \text{ W}/(\text{m}\cdot^\circ\text{C})$ , volumetric specific heat is  $2200 \text{ kJ}/(\text{m}^3\cdot^\circ\text{C})$  and the thermal conductivity of the spiral pipe is  $0.45 \text{ W}/(\text{m}\cdot^\circ\text{C})$ .

2.3.2. Effect of pile diameter on heat transfer performance

Figure 9a shows the effect of pile diameter on heat flux per unit pipe length of the pile. The analysis shows that with the increase of pile diameter, the heat flux per unit pipe length decreases gradually, but the variation range is relatively small, which indicates that although the increase of pile diameter will cause the length of the spiral pipe to increase approximately proportionally, however, due to the increase of pile diameter, the phenomenon of thermal short circuit in the backfill area is weakened, which will weaken the influence on heat flux per unit pipe length. Taking the pile depth  $H = 8 \text{ m}$  as an example, pitch  $b$  is, respectively, 0.1 and



(a)

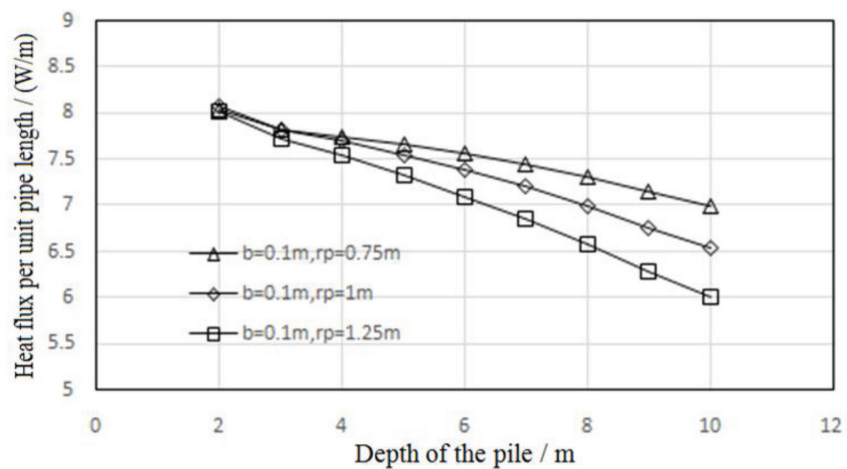


(b)

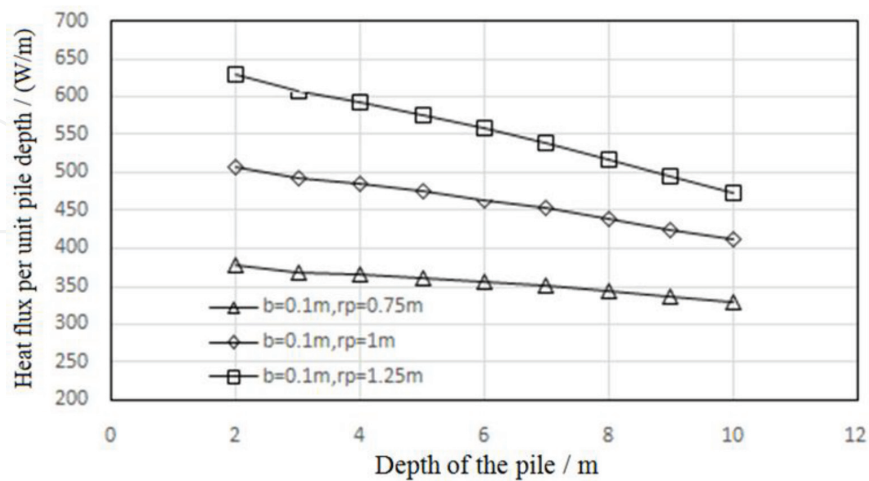
Figure 9. Effect of pile diameter on heat transfer performance. (a) Heat flux per unit pipe length. (b) Heat flux per unit pile depth.

0.3 m; when the pile diameter increases from 1 to 2.5 m, the average heat flux per unit pipe length decreases from 7.28 to 6.58 W/m, from 17.30 to 15.36 W/m, a relative decrease of 9.6 and 11.2%, respectively. The pile diameter increases by 0.1 m. The average heat flux per unit pipe length decreases by 0.047 and 0.129 W/m, respectively.

**Figure 9b** shows the effect of pile diameter on the heat flux per unit pile depth of the pile. It can be seen from the figure that with the increase of pile diameter, the heat flux per unit pile depth increases approximately linearly, which is due to the increase of buried pipe length, that is, the contact area between spiral buried pipe and surrounding area increases, resulting in the heat transfer amount of the pile greatly increasing; thus, the heat flux per unit pile depth increases approximately linearly in proportion. Taking the pile depth  $H = 8$  m as an example, the pitch  $b$  is, respectively, 0.1 and 0.3 m; when the pile diameter increases from 1 to 2.5 m, the average heat flux per unit pile depth increases from 228.8 to 516.3 W/m, from 182.0 to 402.3 W/m, an increase of 1.26 times and 1.21 times, respectively. The pile diameter increases by 0.1 m. The average heat flux per unit pile depth increases by 19.2 and 14.7 W/m, respectively.



(a)

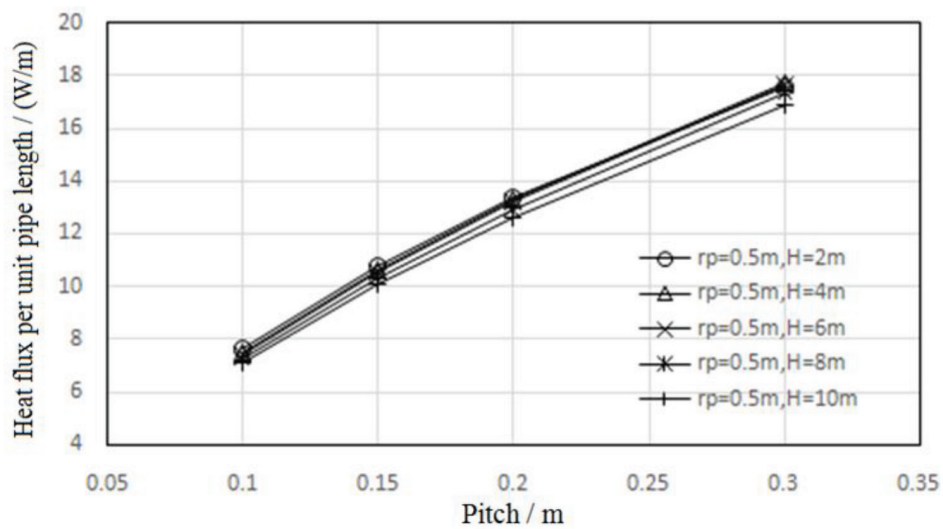


(b)

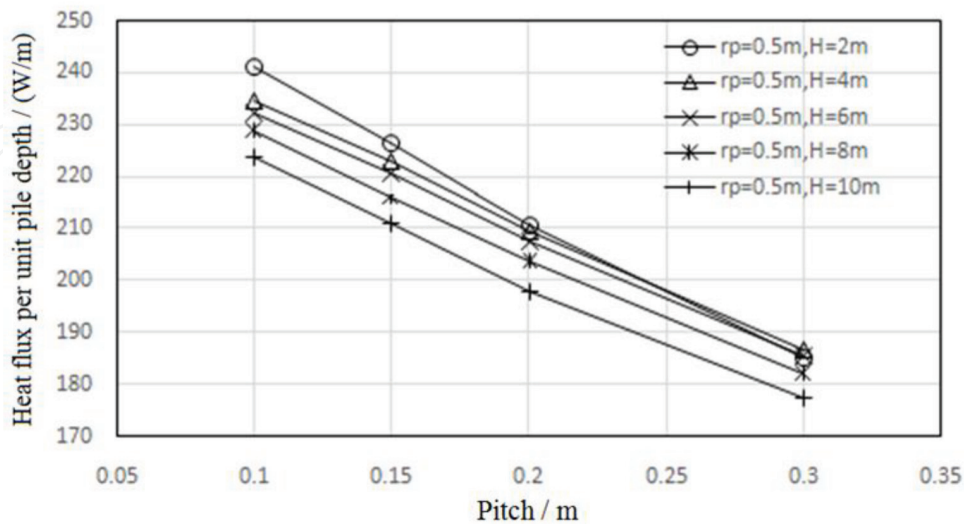
**Figure 10.** Effect of pile depth on heat transfer performance. (a) Heat flux per unit pipe length. (b) Heat flux per unit pile depth.

### 2.3.3. Effect of pile depth on heat transfer performance

**Figure 10** shows the effect of different pile depths on the heat transfer performance under different pile diameters with pitch  $b = 0.1$  m. As can be seen from the figure, with other conditions constant, the deeper the heat transfer pile, the longer the tube length, the lower the outlet temperature, the smaller the average heat transfer temperature difference and the smaller the heat flux per unit pipe length; at the same time, the increase of the pile depth will further increase the speed of the decrease of the heat flux per unit pipe length. Taking pile radius  $r_p = 0.75$  and  $1.2$  m as an example, the heat flux per unit pipe length decreases from  $8.03$  to  $6.99$  W/m and  $8.02$  to  $6.02$  W/m when the pile depth  $H$  increases from  $2$  to  $10$  m, a decline of  $12.9$  and  $25.0\%$ , respectively.



(a)



(b)

**Figure 11.** Effect of pitch on heat transfer performance. (a) Heat flux per unit pipe length. (b) Heat flux per unit pile depth.

Similarly, for the heat flux per unit pile depth, due to the increase of pile depth, resulting in lower average heat transfer temperature difference, heat flux per unit pile depth decreases. In addition, under different pile diameter conditions, the difference of heat flux per unit pile depth is larger, and the larger the pile diameter, heat flux per unit pile depth decreases. Taking  $r_p = 0.75$  and  $1.25$  m as an example, when pile depth  $H$  increases from 2 to 10 m, the heat flux per unit pile depth decreases from 378.3 to 329.2 W/m and from 629.6 to 472.2 W/m, a decline of 12.9 and 25.0%, respectively.

#### 2.3.4. Effect of pitch on heat transfer performance

**Figure 11** shows the effect of pitch on heat transfer performance. Analysis finds that the pitch has greater impact on the heat flux per unit pipe length. Due to the increase of the pitch, the distance between the spiral tubes increases, and the axial short circuit phenomenon of the adjacent spiral tubes is weakened; thus, the heat flux per unit pipe length increases. Taking the pile radius  $r_p = 0.5$  m as an example, when the pile depth  $H = 8$  m, the pitch increases from 0.1 m to 0.3 m; the heat flux per unit pipe length increases from 7.28 to 17.31 W/m, an increase of 1.38 times. For each 0.1 m increase in pitch, the heat flux per unit pipe length increases by an average of 3.34 W/m.

Although the heat flux per unit pipe length increases approximately linearly with the increase of pitch, the heat flux per unit pile depth is approximately linearly reduced. The increase of pitch will reduce the axial thermal short circuit; thus, the effective heat transfer tube length is reduced for a certain size of the energy pile, that is, the effective heat transfer area of the fluid and the soil is reduced; thus, the total heat transfer amount of the pile is reduced. Taking the pile radius  $r_p = 0.5$  m as an example, when the pile depth  $H = 8$  m, the pitch increases from 0.1 to 0.3 m; the heat flux per unit pile depth decreases from 228.8 to 182.0 W/m, decreases by 20.5%. For every 0.1 m increase in pitch, the heat flux per unit pile depth has an average of 15.6 W/m decrease.

### 3. Conclusion(s)

Both the analytical solution model and numerical solution model for CyHEP are built to discuss their dynamic characteristics of thermal interferences and heat transfer performance. The following conclusions can be drawn.

1. Four heat exchange stages for the spiral pile geothermal heat exchanger along the fluid flow direction are revealed: inlet heat exchange stage, grout thermal short-circuiting stage, small temperature difference stage and outlet heat exchange stage. Each stage has corresponding heat transfer characteristics, and reducing the length of small temperature difference stage and increasing the other stages would enhance the heat exchange of spiral geothermal ground heat exchanger.
2. As the pile diameter increases, the heat transfer per unit tube length decreases, and the heat exchange per unit pile depth increases. For every 0.1 m increase in pile diameter, the



heat transfer per unit tube length decreases by an average from 0.047 to 0.129 W/m, and the unit heat exchange per unit pile depth increases by 14.7 to 19.2 W/m.

3. As the pile depth increases, the heat transfer per unit tube length and the heat exchange per unit pile depth are reduced. During the process of increasing  $H$  from 2 m to 10 m, the heat exchange per unit tube length and the heat exchange per unit pile depth are reduced from 1.04 to 2.00 W/m and 49.1–157.4 W/m, respectively.
4. As the pitch increases, the heat transfer per unit tube length increases, and the heat exchange per unit pile depth decreases. For a 0.1 m increase in pitch, the heat transfer per unit tube length increases by 3.34 W/m, and the unit heat exchange per pile depth decreases by 15.6 W/m.

## Acknowledgements

I would like to express my gratitude to all those who helped me during the writing of this book. And I feel grateful to all the teachers in the Army Logistical University of PLA who once offered me valuable courses and advice during my study. Last, my thanks go to my beloved family for their loving considerations and great confidence in me all through these years. I also owe my sincere gratitude to my friends who gave me their help and time in listening to me and helping me work out my problems during the difficult course of the book.

This work received support from the Research Initiative for Basic Science and Frontier Technology of Chongqing, China [cstc2016jcyjA0496], Natural Science Foundation of China [51706243].

## Conflict of interest

We declare that we have no financial and personal relationships with other people or organizations that can inappropriately influence our work; there is no professional or other personal interest of any nature or kind in any product, service and/or company that could be construed as influencing the position presented in, or the review of, our work.

## Appendices and Nomenclature

$x, y, z$	Cartesian coordinate (m)
$r, \varphi, z$	cylindrical coordinate (m)
$R, \varphi, Z$	dimensionless cylindrical coordinate
$h$	height (m)
$H$	dimensionless height

$r$	radial coordinate (m)
$R$	dimensionless radial coordinate
$q_1$	heating rate per length of pipe ( $W s^{-1}$ )
$\tau$	the time (s)
$\alpha_s$	thermal diffusivity ( $m^{-2} s$ )
$d_p$	distance from the heat source point to the calculated point (m)
$d_n$	distance from the heat sink point to the calculated point (m)
$D_p$	dimensionless distance from the heat source point to the calculated point (m)
$D_n$	dimensionless distance from the heat sink point to the calculated point (m)
$\rho$	density ( $kg m^{-3}$ )
$c$	specific heat ( $J kg^{-1} K^{-1}$ )
$\lambda$	thermal conductivity ( $W m^{-1} K^{-1}$ )
$\Delta T$	the temperature rise (K)
$R$	thermal resistance ( $m^{-1} K^{-1} W$ )
$L$	Length of helix pipe

**Greek symbols**

$\theta$	cone angle (rad)
$\varphi$	spiral angle (rad)
$Fo$	Fourier number
$\eta$	influence coefficient
$\Theta$	dimensionless temperature rise

**Superscript**

'	integration parameter
ave.	the average value
CyHEP	cylinder helix energy pile
CoHEP	truncated cone helix energy pile
t	top surface of pile
b	base surface of pile
mi	middle surface of pile

<i>i</i>	the index of arc
<i>j</i>	the index of coil
<i>k, n</i>	the index of time
p	Pipe
f	fluid
g	ground

## Author details

Guangqin Huang\*, Yajiao Liu, Xiaofeng Yang and Chunlong Zhuang

\*Address all correspondence to: hgq880818@163.com

Department of Military Installation, Army Logistical University of PLA, Chongqing, China

## References

- [1] Hamada Y, Saitoh H, Nakamura M, Kubota H, Ochifuji K. Field performance of an energy pile system for space heating. *Energy and Buildings*. 2007;**37**:517-524. DOI: 10.1016/j.enbuild.2006.09.006
- [2] Gao J, Xu Z, Liu J, Li KS, Yang J. Thermal performance and ground temperature of vertical pile-foundation heat exchangers: A case study. *Applied Thermal Engineering*. 2008;**28**: 2295-2304. DOI: 10.1016/j.applthermaleng.2008.01.013
- [3] Cecinato F, Loveridge FA. Influences on the thermal efficiency of energy piles. *Energy*. 2015; **82**:1021-1033. DOI: 10.1016/j.energy.2015.02.001
- [4] Park H, Lee S-R, Yoon S, Choi J-C. Evaluation of thermal response and performance of PHC energy pile: Field experiments and numerical simulation. *Applied Energy*. 2013;**103**:12-24. DOI: 10.1016/j.apenergy.2012.10.012
- [5] Zarrella A, De Carli M. Heat transfer analysis of short helical borehole heat exchangers. *Applied Energy*. 2013;**102**:1477-1491. DOI: 10.1016/j.apenergy.2012.09.012
- [6] Zarrella A, De Carli M, Galgaro A. Thermal performance of two types of energy foundation pile: Helical pipe and triple U-tube. *Applied Thermal Engineering*. 2013;**2**:301-310. DOI: 10.1016/j.applthermaleng.2013.08.011
- [7] Zarrella A, Capozza A, De Carli M. Analysis of short helical and double U-tube borehole heat exchangers: A simulation-based comparison. *Applied Energy*. 2013;**112**:358-370. DOI: 10.1016/j.apenergy.2013.06.032